AIMS Materials Science, 5(6): 1242–1254.
DOI: 10.3934/matersci.2018.6.1242
Received: 30 June 2018
Accepted: 27 November 2018
Published: 03 December 2018

http://www.aimspress.com/journal/Materials

Research article

Preparation and characterization of nanocarbons from *Nicotiana tabacum* stems

Cabinet Chivimbiso Musuna-Garwe[1], Netai Mukaratirwa-Muchanyereyi[2], Mathew Mupa[2,*], Courtie Mahamadi[2] and Munyaradzi Mujuru[3]

[1] Tobacco Research Board, Department of Analytical Chemistry, P.O. Box 1909, Harare, Zimbabwe
[2] Bindura University of Science Education, Department of Chemistry, Private Bag 1020, Bindura, Zimbabwe
[3] Department of Water and Sanitation, University of Limpopo, P.O. Box X1106, Sovenga 0727, South Africa

*** Correspondence:** Email: mathewmupa@daad-alumni.de.

Abstract: Nanocarbon materials can improve adsoption capacity if the nano size range is optimized during production. In this study, nanocarbons were prepared from green recyclable waste *N. tabacum* stem using carbonization process and KOH as the activating agent, thus potentially unclocking value in the otherwise waste material. The formation of nanocarbons was investigated at different KOH concentration, activation temperature and carbonization time. Fourier Transform Infrared (FT-IR) spectroscopy, X-ray Diffraction (XRD), Scanning Electron Microscopy (SEM), Transmission Electron Microscopy (TEM) and Brunauer–Emmett–Teller (BET) techniques were used to characterise the nanocarbon material. The results showed that nanocarbons with high specific surface areas in excess of 950 m^2/g and nanostructured morphologies characterized by pore width averages ranging from 3.33–8.87 nm, pore diameter 10.59–45.30 nm and particle size 25.34–54.88 nm could be formed. Optimum nanocarbon production was achieved when the precursor was activated using 10% KOH and carbonized at a temperature of 400 °C for 4 h. Characteristic FT-IR absorption bands were observed in all carbonized samples. SEM images revealed a dense irregular material with cavities and protuberances. XRD patterns showed that crystallinity of the nanocarbons decreased with increase in carbonization time. The properties reported for the nanocarbons are ideal for adsoption of analytes from complex matrices, hence presenting *N. tabacum* as a promising low-cost and green alternative precursor for nanocarbon production targeting analytical fields such as solid-

phase extraction and solid phase microextraction. The produced nanocarbons appear to be carbon nanoparticles comprising nearly spherical particles.

Keywords: nanocarbons; *Nicotiana tabacum*; carbonization time; surface morphology; green technology

1. Introduction

Increasing industrial activities have led to a search for materials that are readily available, effective, cheap and renewable. Research has thus been emphasizing on the recycling and re-use of agricultural wastes for the production of valuable products. This has seen the production of carbonaceous nano-structured materials from bio-waste gaining momentum due to the materials' wide applications [1]. Recently, research on nanocarbon formation has mainly been centered on the biomass source, formation process and identification of the final product composition [2]. Many production processes have been developed and applied. These include the catalytic and hydrothermal carbonization (HTC) processes, pyrolysis, electric arc discharge, laser ablation, float catalysis and chemical vapor deposition [3–5]. The HTC process has been used on many agricultural waste bi-products which include rice husks [6], peach stones [7] and cashew nut shell [8]. The activation process has mainly been achieved through the use of chemical process with agents such as $ZnCl_2$, KOH and H_3PO_4 being the most popular [9].

N. tabacum stems are agricultural wastes which have not been beneficially used, despite the huge volumes produced each year world-wide. However, a greater proportion (approximately two-thirds of cell wall dry matter) of *N. tabacum* stems are carbohydrate polymers (cellulose and hemicellulose) which places them as perfect candidates for the preparation of nanocarbon materials. It is not suprising therefore, that several workers have studied their potential applications in many fields. Peševski et al. alluded to the possibilities of producing energy briquettes from *N. tabacum* stems [10]. Graciano et al. identified the best parameters for the simultaneous saccharification and fermentation process of *N. tabacum* stems as an attractive raw material for the production of ethanol [11]. *N. tabacum* stems have also been applied in the form of *N. tabacum* dust [12], *N. tabacum* stem ash [13] and as plain *N. tabacum* stems [14] for the adsorption of metals and organic impurities in water. Li et al. prepared carbon material from *N. tabacum* stems using potassium carbonate and phosphoric acid as activation agents [15].

There is evidence in the literature which show that activated carbon prepared by KOH activation is highly microporous and has an enhanced surface area when compared to that produced through $ZnCl_2$ or H_3PO_4 activation [16,17]. However, it is also evident that limited work has been reported on the use of *N. tabacum* as a precursor for the production of nanocarbons and to the best of our knowledge, preparation of nanocarbon materials from *N. tabacum* stems using KOH as an activation agent at low temperatures has not been reported.

The aim of this study was therefore to use *N. tabacum* stems as a precursor to engineer self-assembled nanocarbons of below 50 nm in nanosize, which are mesoporous with a high surface area. The production process was optimsed with respect to KOH concentration, carbonization time and carbonization temperature. The surface morphology and functional group composition were carefully investigated using the BET, Iodine number, SEM, TEM, XRD techniques and FT-IR to assess the

suitability of the nanocarbons for potential application in analytical fields as clean up material for analytes in complex matrix.

2. Materials and methods

2.1. Preparation of nanocarbon preparation

Wet *N. tabacum* stems harvested from a Tobacco Research Board's Kutsaga Research Station plot were cleaned, chopped to 20–30 cm pieces and placed in a drying room maintained at a temperature of 105 ℃ for three days. The dried stems were then ground with a mechanical grinder and sieved through a mesh size of ~2 mm. Triplicates of ground tobacco samples (10 g) placed in crucibles were each impregnated with 40 mL of 10% KOH over period of 24 h. The crucibles were then placed in a muffle furnace and pre-purged with nitrogen gas to create an inert atmosphere. The temperature was gradually increased at 5 ℃ intervals to required setting according to the experimental design in Table 1 with continuous purging with inert gas. After each cycle, the samples were allowed to cool in desiccators and then washed with 0.1 M HCl. This was followed by washing with hot de-ionized water and then cold de-ionized water until a pH of ~6.5 was attained. Samples were finally dried in an oven at 105 ℃ before they were characterized.

From the four operational parameters in Table 1, an L_{12} orthogonal array [18] was used to evaluate the optimal values as shown in Table 2.

Table 1. Carbonization-activation process parameters.

Independent variable	Range and values				
	Sample	1	2	3	4
Concentration of KOH (Vol %)	A	10	30	50	70
Carbonization temperature (℃)	B	250	300	400	500
Carbonization time (hours)	C	2	3	4	5

Table 2. Operational parameters in L_{12} orthogonal array.

Sample ID	Variables		
	A	B	C
1	1	1	1
2	2	1	1
3	3	1	1
4	4	1	1
5	1	1	1
6	1	2	1
7	1	3	1
8	1	4	1
9	1	1	1
10	1	1	2
11	1	1	3
12	1	1	4

2.2. Characterisation of the nanocarbons

The iodine number of the sample was determined using an ASTM method for the determination of iodine number of carbon material [19]. The specific gravity was determined using a pycnometer, while the ash content was determined by igniting dried stems in a muffle furnace at 550 ℃. The carbon content was determined using the ashing method at 550 ℃ in a muffle furnace.

FTIR analyses were done using a Perkin-Elmer Spectrum 100 spectrophotometer. Each sample was mixed with KBr and pressed into a pellet. The spectra were recorded in the MIR region from 500 cm^{-1} to 4000 cm^{-1} with a spectral resolution of 4 cm^{-1}.

X-ray powder diffraction patterns of the nanocarbons were recorded on an XPERT PRO PANalytical X-ray diffractometer for phase identification. The patterns were run with CuKα radiation with a secondary monochromator (λ = 0.1545 nm) at 45 kV and 40 mA. The diffraction measurements were conducted at room temperature in a Bragg-Brenton geometry with a scan range of 2θ = 5–90 °using continuous scanning at a rate of 0.02 ⁰/s.

The surface morphology of the nanocarbons was studied using FE SEM (JEOL 7500F SEM) at 2 kV accelerating voltage. The sample was sputter coated with carbon to avoid surface charging.

Structural analysis was done on the TEM (JEOL) 2100 in which the sample was ground in a pestle and mortar and a suspended in acetone. A small volume of this suspension was then placed in a hole of carbon film supported on a copper grid to allow the direct transmission of the electron beam.

The particle porosity of the nanocarbons was determined using an automatic chemisorption and physisorption analyser with N_2 being the adsorbate at 77.3 K. The specific surface area and total pore volume were calculated from the Brunauer–Emmett–Teller (BET) equation, whereas the microporosity and mesoporosity were determined using the v–t and the Barrett–Joyner–Halenda (BJH) methods respectively.

3. Results and discussion

3.1. Physicochemical properties of ground N. tabacum stems

A proximate analysis of the ground *N. tabacum* stems showed a carbon content of 51%. This high carbon content ensured the feasibility of producing nanocarbons from this substrate. The material had a low ash content of 4.47% which is also ideal for nanocarbons production. The effect of carbonization temperature, time and concentration of KOH on the average % yield and iodine number is illustrated in Figure 1. As the KOH concentration is increased, there is a decline in both the yield and iodine number. However, the yield and iodine number increased as carbonization time was increased from 2 h to 4 h. This may have been as a result of increased carbonization as the precursor material is exposed to more carbonization time. Beyond the 4 h, however, there tends to be a decline in both the yield and iodine number. This might be due to the burning off, of the produced nanocarbons beyond the optimum 4 h.

An increase in carbonization temperature from 250 ℃ to 400 ℃ resulted in an increase in the nanocarbons yield and iodine number. When the temperature was however, increased to 500 ℃, both parameters declined showing that the nanocarbons were being burnt off and some of the produced pores collapsing closing the pores impacting on both yield and the iodine number.

The optimum operating conditions based on the iodine number and yield were found to be a carbonization temperature of 400 ℃, a carbonization time of 4 h and an impregnating solution of 10% KOH. High iodine number of above 1000 is an indicator of high surface area of the material which is a positive characteristic in as far as sample clean-up use is concerned.

Further characterization work was done using the 10% KOH at 400 ℃ but varying the carbonization time from 2 h, 3 h to 4 h to see the effect of time on the produced material character. These samples were labeled A, B and C respectively in the following characterization results.

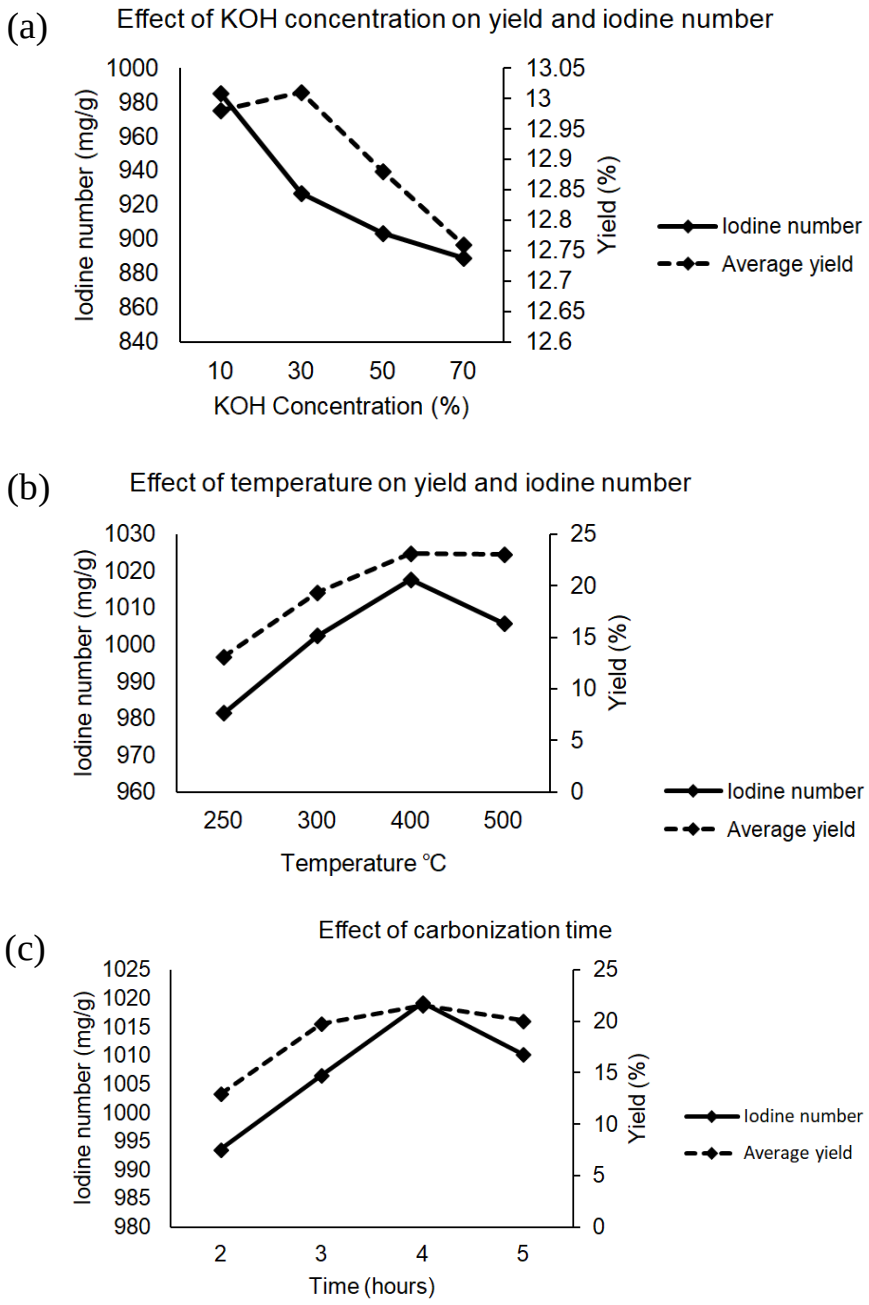

Figure 1. Operational parameters effects on the responses of nano-carbon prepared from tobacco stems: (a) concentration of KOH, (b) carbonization temperature (℃) and (c) carbonization time (hours).

3.2. Results from instrumental characterization

FTIR technique is used to identify functional groups of a material. The presence of certain functional groups enables one to elucidate adsorption mechanisms in SPE sample clean-up or any adsorption process and to adapt experimental conditions for the removal of certain organic compounds. Figure 2 shows FT-IR spectra of the nanocarbons under specified conditions. The spectra indicate the presence of expected functional groups, which are given in Table 3. As the carbonization time was changed, the spectra revealed either a disappearance, reduction or broadening of the peaks. This showed that carbonization time affected the spectra characteristics of the produced material. The material carbonized for 4 h exhibiting typical peaks although broader.

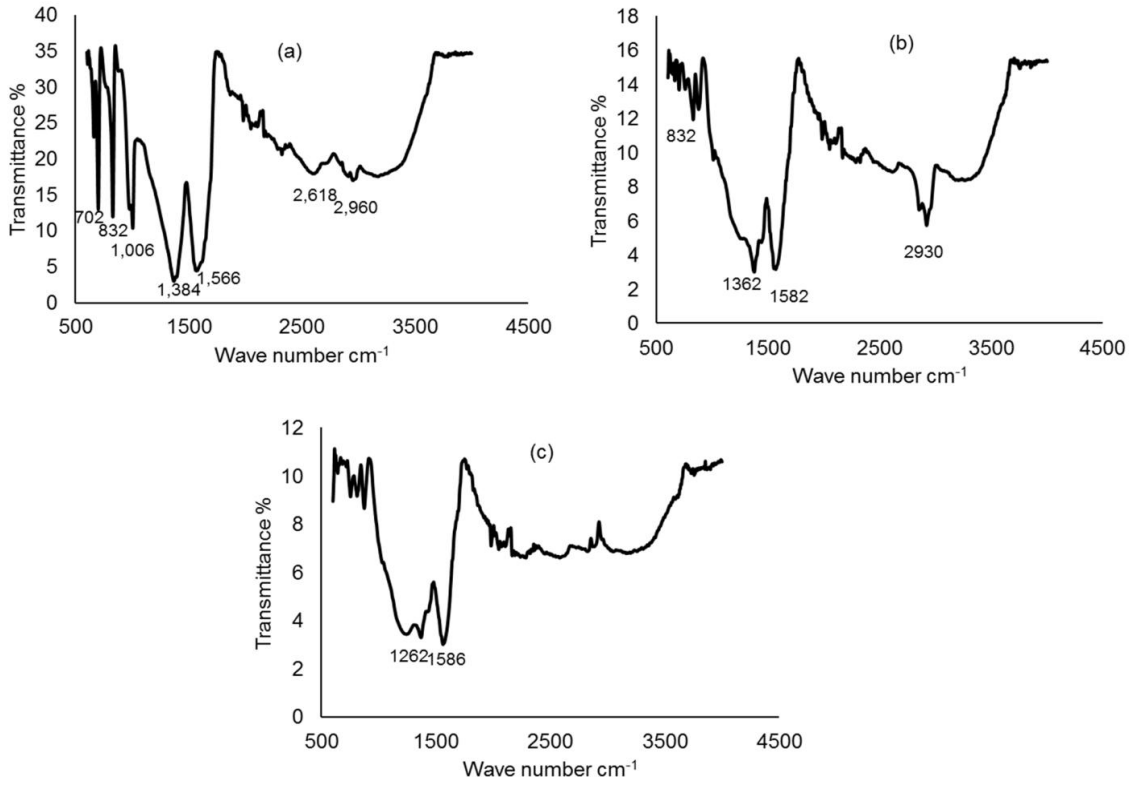

Figure 2. FT-IR spectra of nano-carbons carbonized at 400 ℃ for (a) 2 h, (b) 3 h and (c) 4 h.

Table 3. A comparison of FTIR absorption bands assignment for the samples and effect of parameter variations.

Assignment	Band Position (cm^{-1})			References
	A	B	C	
C–H bend	701	-	-	[19]
C–H bend	832	832	-	[19]
C–O stretch	1006	-	-	[19]
C–H stretch in alkanes	1384	1362	1262	[19]
C=C vibrations	1566	1582	1586	[20]
C–H vibration	2960	2930	-	[21]

Cao et al. observed peaks at 1008 cm^{-1} which they assigned to C–O vibration in pure multi-walled carbon nanotubes (MWCNTs) [20]. MWCNT have been found to have clean-up adsorption properties [20–23].This shows that this product may have some MWCNT. However, this peak became small as the carbonization time increased and subsequently disappeared after 4 h. Also the C=C at band position 1586 cm^{-1} for material carbonized at 4 h signifies a move toward nanocarbon material. These MWCNT and the C=C characteristics of the produced materials may be useful in sample clean up adsorbent properties.

Surface area has a strong effect on the physical and chemical properties on any adsorbent material critical in sample clean up. The microstructure of produced materials were examined by SEM and the images of nanocarbons shown in the Figure 3.

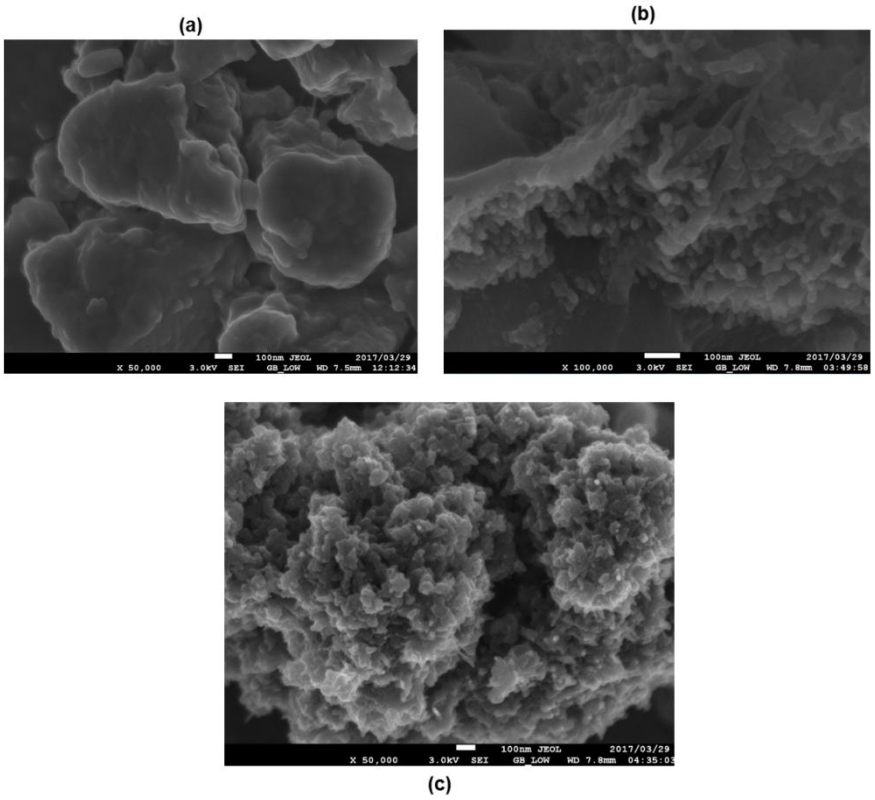

Figure 3. SEM images for nanocarbons carbonized at 400 ℃ for (a) 2 h, (b) 3 h and (c) 4 h.

The SEM micrographs suggest that the material has non regular compacted surface with cavities and protuberances. This could be due to breakdown of the lignocellulosic material and evaporation of volatile compounds that leave the nanocarbons with well developed pores. The SEM micrographs show that vesicles and spaces within the nanocarborns are of micropore size and do not contribute to the adsoption capacity of the nanocarbons. Similar findings were reported by Rodriguez and others, reported that such visicles and spaces do not attract the sorbate molecules towards them but that once the adsorbate comes into contact with the surface of microporosity, then adsorption occurs and the adsorbate molecules enter the micropore network [24]. Mesopores were also observed in this study. Hu et al. also alluded to both mesopores and micropores being formed as a result of the incorporation of K into the C network [25]. There is enlarging of the pores of biomass with increase in exposure

time at 400 ℃. A study by some researchers established that surface area of nanocarbons does increase with increase in activation temperature because activation reactions occur faster at higher temperatures and more pore channels are developed accordingly indicating the importance of temperature in developing mesopores [25] which are ideal for sample clean-up. This was also observed in the present study coloborating the iodine numbers in the same study. The nanocarbons micrographs suggest they are porous, a result which is similar to what has been previously reported [26].

The TEM method used in this research only provided the structural analysis in which the images were created by adsorption effects. From Figure 4, one can observe that the TEM micrographs of the produced nanocarbons showed spherical orientation. These produced nanocarbons appear to be carbon nanoparticles comprising nearly spherical particles with diameters below 100 nm which are agglomerated clusters [27]. Gasification has produced cavities of mesopore size ideal for sample clean-up. Marsh et al. highlighted that it was difficult to distinguish nanocarbons prepared by thermal activation from those prepared by chemical activation [28]. The BET nano-sizes ranging from 54.88 to 25.34 are in agreement with reports from other workers [29], with the 25.34 nm particles being the most ideal for sample clean-up. This was calculated from d_{BET} fomular of 6000/ns, where n is is the theoretical density and s is the specific surface area and thus is being compared to 27 nm which is the surface area diameter based on gas adsorption surface area analysis (BET) [29]. Observed size in this research was also confimed by the observed TEM images (Figure 4a,b). Although the TEM are larger than the BET calculated sizes, similar trends were observed by other researchers [29]. The SEM images however, appeared to be in agreement with the TEM images.

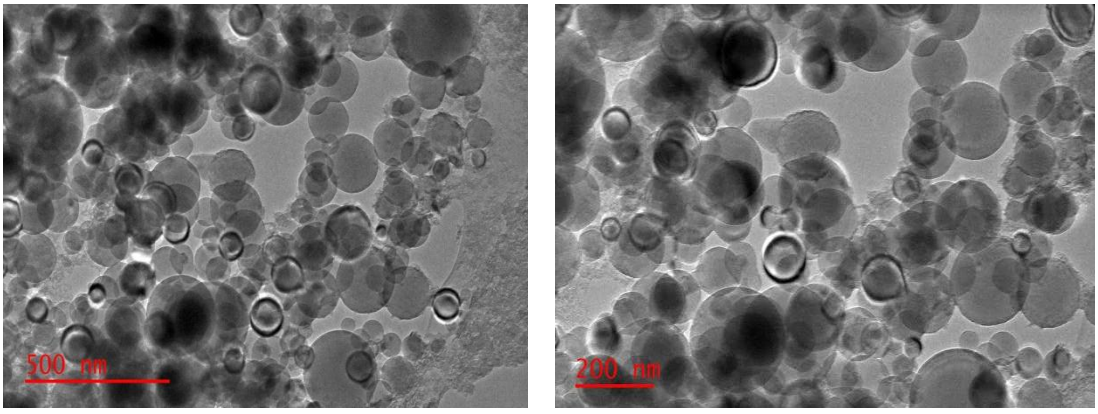

(a) (b)

Figure 4. TEM images for nanocarbons carbonized at 400 ℃ for 4 hours.

Figure 5 shows the results for the three samples analysed by XRD. The three diffractograms in Figure 5a–c show a progressive clean up of the nanocarbons with increase in exposure time at 400 ℃. Crysrallinity of the nanocarbons decreased with increasing carbonization time. The two broad peaks at around 23 ° and 43 ° correspond to (002) and (100) planes respectively and confirm the amorphous nature of the nanocarbon which is useful during sample-clean up. The sharp peak at around 26 ° confirms the presence of carbon material [30]. This carbon peak had highest intensity in the sample prepared at 400 ℃ and carbonized for 4 hours.

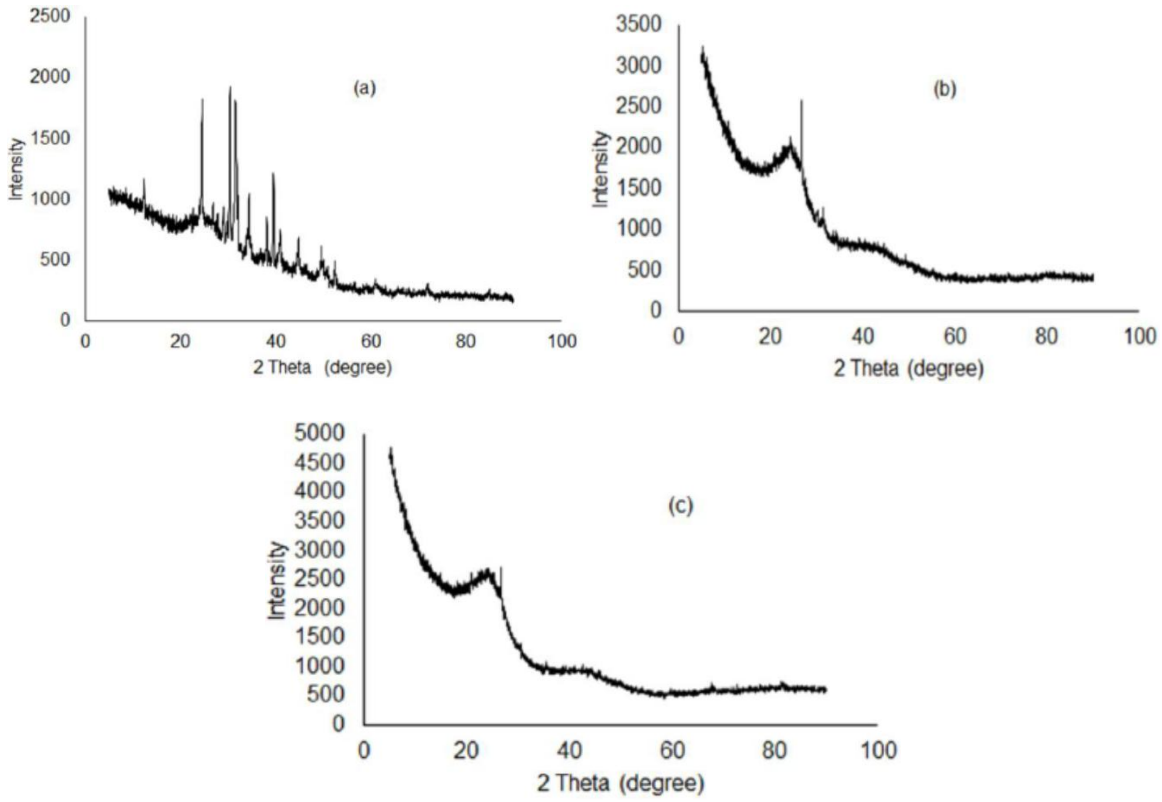

Figure 5. XRD of nanocarbons carbonized at 400 ℃ for (a) 2 h, (b) 3 h and (c) 4 h.

3.3. BET surface area analysis

Surface area is an important parameter for any adsorbent material as it is directly proportional to accessible active sites. Nanocarbons have larger surface areas of greater than 900 m^2/g. The isotherm shapes in Figure 6 can be classified as a type II character according to the International Union of Pure and Applied Chemistry (IUPAC) classification. This is an indication that the nanocarbons are more of mesoporous. The result is in aggrement with the observation that mesoporous nanocarbons are produced when KOH is used as an impregnating material [31]. The figure indicate that the material porosity increased with increase in time of carbonization, making the nanocarbons prepared at 4 h ideal for sample matrix clean-up.

It has been reported that the reactions which occur during thermal carbonization of biomass are very complicated [31]. They involve hydrolysis, dehydration, decomposition and condensation. The thermal process hydrolyses lignin and hemicelluloses, reduces the crystallinity of cellulose and enlarges the pores of biomass. The surface areas were found to be 454.63 m^2/g, 678.02 m^2/g and 984.59 m^2/g (Table 4) for exposure times of 2 h, 3 h and 4 h respectively. Surface area increased with increase in carbonization time which is ideal for sample clean-up. The larger the surface area the less adsorbent material is needed for sample clean up making the technique more environmentally friendly. The pore volume were found to be 0.41 cm^3/g, 0.47 cm^3/g and 0.63 cm^3/g for the 2 h, 3 h and 4 h exposure times respectively. These results are in agreement with the increase in iodine numbers with carbonization time that were observed. The iodine numbers were found to 993.57, 1006.57 and 1019.29 for 2 h, 3 h and 4 h respectively.

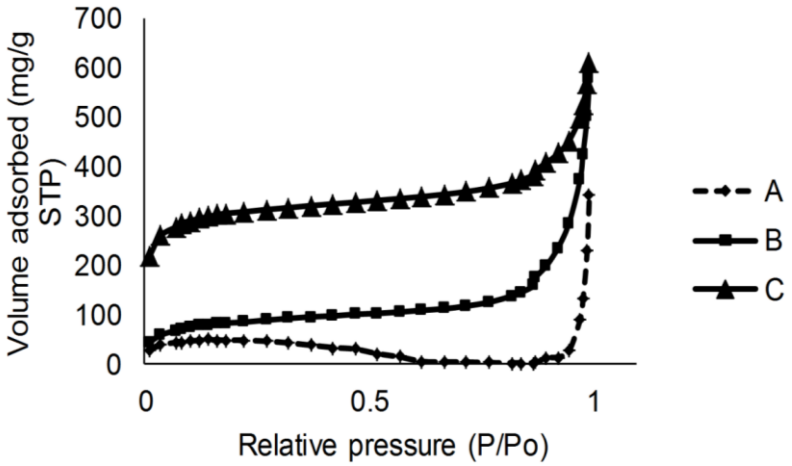

Figure 6. N_2 adsorption isotherm at 77.3 K of tobacco stem based nanocarbons A is sample carbonized at 400 ℃ for 2 hours, B is sample carbonized to 400 ℃ for 3 hours and C is sample carbonized to 400 ℃ for 4 hours.

Table 4. BET parameters of the nanocarbon.

Parameter	A	B	C
S_{BET} (m^2/g)	454.63	678.02	984.59
BET constant (C)	80.93	123.14	145.49
R^2	0.996	0.999	0.999
Pore volume (cm^3/g)	0.41	0.47	0.63

3.4. Pore size distribution

The micropore size analysis was done using the (v–t) method. The mesopore size distribution analysis was done using the Barrett–Joyner–Halenda (BJH) method. Table 4 shows the micropore parameters and mesopore size distribution.

Table 5. Surface area and pore characteristics of the samples.

Parameter	A	B	C
Micropore volume (cm^3/g)	0.31	0.46	0.63
Micropore area (m^2/g)	161.96	241.32	352.34
External surface area (m^2/g)	325.93	485.63	709.02
Total surface area (m^2/g)	454.65	678.02	984.59
Pore width (nm)	8.87	10.22	3.33
Pore diameter (nm)	45.30	22.29	10.59
Particle size (nm)	54.88	36.80	25.34

The average pore width distribution initially increased before decreasing as the carbonization time was increased from 2–4 h. However, workers elsewhere reported a decrease in average pore width size distribution with increase in carbonization time [29]. The anomaly could be attributed to

non homogenous nature of the sample particles. Particle size, pore diameter and pore width decrease are characteristics that are useful in sample matrix clean-up since the lower they are, the more efficient the sample clean-up. The values of parameters presented in Table 5 fall withing the typical ranges ideal for efficient analyte adsorption.

4. Conclusion

A simple, green approach for the production of nanocarbons using an agricultural waste (*N. tabacum*) is reported in this study. The production process was found to occur optimally when using a 10% KOH solution as the activating agent and carbonizing at a temperature of 400 ℃ for 4 h. Instrumental characterization of the nanocarbons using BET, FT-IR, SEM, TEM and XRD techniques showed that the nanocarbons had high surface area (BET value > 950 cm^2/g and iodine number > 1000 mg/g), amorphous with cavities, protuberances, micropores and mesopores. The range of the surface characterization parameters indicated that the *N. tabucum* could be a green source for low-cost production of nanocarbons with vast potential for applications in sample clean-up. The produced nanocarbons type appear to be nearly spherical and may be classified as carbon nanopheres.

Acknowledgements

Authors would like to acknowledge the Tobacco Research Board, Zimbabwe for funding this work.

Conflict of interest

The authors declare no conflict of interest.

References

1. Madhu R, Palanisamy S, Chen SM, et al. (2014) A low temperature synthesis of activated carbon from the bio waste for simultaneous electrochemical determination of hydroquinone and catechol. *J Electroanal Chem* 727: 84–90.
2. Hui TS, Zaini MAA (2015) Potassium hydroxide activation of carbon: a commentary. *Carbon Lett* 16: 275–280.
3. Ravelo-Pérez LM, Herrera-Herrera AV, Hernandez-Borges J, et al. (2010) Carbon nanotubes: Solid-phase extraction. *J Chromatogr A* 1217: 2618–2641.
4. Li X, Xing W, Zhuo S, et al. (2011) Preparation of capacitor's electrode from sunflower seed shell. *Bioresource Technol* 102: 1118–1123.
5. Ashokumar M, Narayanan NT, Gupta BK, et al. (2013) Conversion of industrial bio-waste into useful nanomaterials. *ACS Sustain Chem Eng* 1: 619–626.
6. Rahman MA, Amin SMR, Alam AMS (2012) Removal of methylene blue from waste water using activated carbon prepared from rice husk. *Dhaka Univ J Sci* 60: 185–189.
7. Álvarez-Torrellas S, García-Lovera R, Rodríguez A, et al. (2015) Removal of methylene blue by adsorption on mesoporous carbon from peach stones. *Chem Eng Trans* 43: 1963–1968.

8. Mohan MA, Chadaga M (2014) Methylene blue colour removal using physically and chemically activated cashew nut shell activated carbon. *IJTEEE* 2: 64–69.
9. Molina-Sabio M, Rodriguez-Reinoso F (2004) Role of chemical activation in the development of carbon porosity. *Colloid Surface A* 241: 15–25.
10. Peševski MĐ, Iliev BM, Živković DL, et al. (2010) Possibilities for utilization of tobacco stems for production of energetic briquettes. *J Agr Sci* 55: 45–54.
11. Graciano RML, de Freitas VP, Ábel FM (2014) Simultan sacharification and fermentation of tobacco samples. *Analecta Technica Szegedinensia* 8: 80–89.
12. Qi BC, Aldrich C (2008) Biosorption of heavy metals from aqueous solutions with tobacco dust. *Bioresource Technol* 99: 5595–5601.
13. Ghosh RK, Reddy DD (2013) Tobacco stem ash as an adsorbent for removal of methylene blue from aqueous solution: equilibrium, kinetics, and mechanism of adsorption. *Water Air Soil Poll* 224: 1582.
14. Wang X, Ouyang Y, Li X, et al. (2008) Room-temperature all-semiconducting sub-10-nm graphene nanoribbon field-effect transistors. *Phys Rev Lett* 100: 206803.
15. Li W, Zhang LB, Peng JH, et al. (2008) Preparation of high surface area activated carbons from tobacco stems with K_2CO_3 activation using microwave radiation. *Ind Crop Prod* 27: 341–347.
16. Abechi SE, Gimba CE, Uzairu A, et al. (2013) Preparation and characterization of activated carbon from palm kernel shell by chemical activation. *Res J Chem Sci* 3: 54–61.
17. Viswanathan I, Neel P, Varadarajan TK (2009) Methods of activation and specific applications of carbon materials. National Centre for Catalysis Research, Indian Institute of Technology Madras, Chennai 600 036.
18. Makeswari M, Santhi S (2013) Optimization of preparation of activated carbon from *Ricinus communis* leaves by microwave-assisted zinc chloride chemical activation: Competitive adsorption of Ni^{2+} ions from aqueous solution. *J Chem* 2013: 314790.
19. ASTM D4607-94 (2006) Standard Test Method for Determination of Iodine Number of Activated Carbon. American Society for Testing and Materials, Annual book of ASTM standards.
20. Cao W, Hu SS, Ye LH, et al. (2015) Trace-chitosan-wrapped multi-walled carbon nanotubes as a new sorbent in dispersive micro solid-phase extraction to determine phenolic compounds. *J Chromatogr A* 1390: 13–21.
21. Purkayastha MD, Manhar AK, Mandal M, et al. (2014) Industrial waste-derived nanoparticles and microspheres can be potent antimicrobial and functional ingredients. *J Appl Chem* 2014: 171427.
22. Deng XJ, Guo QJ, Chen XP, et al. (2014) Rapid and effective sample clean-up based on magnetic multiwalled carbon nanotubes for the determination of pesticide residues in tea by gas chromatography–mass spectrometry. *Food Chem* 145: 853–858.
23. Hou X, Lei SR, Qui ST, et al. (2014) A multi-residue method for the determination of pesticides in tea using multi-walled carbon nanotubes as a dispersive solid phase extraction absorbent. *Food Chem* 153: 121–129.
24. Rodriguez-Reinos F, Molina-Sabio M, Gonzalez MT (1995) The use of steam and CO_2 as activating agents in the preparation of activated carbons. *Carbon* 33: 15–23.
25. Hu B, Wang K, Wu LH, et al. (2010) Engineering carbon materials from the hydrothermal carbonization process of biomass. *Adv Mater* 22: 813–828.

26. Senthilkumar ST, Selvan RK (2013) The biomass derived activated carbon for supercapacitor. *AIP Conf Proc* 1538: 124–127.
27. Strachowski P, Bystrzejewski M (2015) Comparative studies of sorption of phenolic compounds onto carbon-encapsulated iron nanoparticles, carbon nanotubes and activated carbon. *Colloid Surface A* 467: 113–123.
28. Marsh H, Rodriguez-Reinoso F (2006) SEM and TEM Images of Structures in Activated Carbons, In: *Activated Carbon*, 1st edition, Elsevier, 366–382.
29. Akbari B, Tavandashti MP, Zandrahimi M (2011) Particle size characterization of nanoparticles—A Practical approach. *IJMSE* 8: 48–56.
30. Hashim M, Sa'adu L (2014) A flexible solid state EDLC from a commercially prepared multiwalled carbon nanortubes and hybrid polymer electrolyte. *J Mater Sci Res* 3: 13–21.
31. Wang HL, Xu ZW, Kohandehghan A, et al. (2013) Interconnected carbon nanosheets derived from hemp for ultrafast supercapacitors with high energy. *ACS Nano* 7: 5131–5141.